Journal of Modern Optics

ISSN: 0950-0340 (Print) 1362-3044 (Online) Journal homepage: http://www.tandfonline.com/loi/tmop20

Single-photon determination of transmission, index of refraction and material thickness

Jin Wang & Shawn Strausser

To cite this article: Jin Wang & Shawn Strausser (2012) Single-photon determination of transmission, index of refraction and material thickness, Journal of Modern Optics, 59:4, 381-386, DOI: 10.1080/09500340.2011.628762

To link to this article: https://doi.org/10.1080/09500340.2011.628762

Journal of Modern Optics
Vol. 59, No. 4, 20 February 2012, 381–386

Taylor & Francis
Taylor & Francis Group

Single-photon determination of transmission, index of refraction and material thickness

Jin Wang* and Shawn Strausser

Physics, Department of Natural Sciences, The University of Michigan, Dearborn, MI 48128, USA

(*Received 9 August 2011; final version received 26 September 2011*)

This paper describes how single photons of light can be used to determine the index of refraction and material thickness. The results of single-photon transmission and polarization interferometer experiments are analyzed to find the index of refraction and thickness of a microscope coverslip. The single photons were generated using non-collinear spontaneous down-conversion. The experimental results are in good agreement with derived theoretical models. This method of determining optical parameters at the quantum level may be useful in performing non-destructive measurements of light-sensitive samples with high precision.

Keywords: optical instrumentation and technology; interferometer; index of refraction; material thickness; single photon

1. Introduction

Research into techniques to improve the measurement of the index of refraction of optical materials is of recent interest [1,2]. Methods to accurately determine the index of refraction are important to quickly evaluate new materials. The ability to measure macroscopic optical properties with a minimum light intensity is useful in measuring light-sensitive samples such as bacteria, DNA, living tissue (eyes), photoresist (used in photolithography), and silver halide salts (used in photographic film), etc. The method presented in this article to determine optical constants using single photons can also be applied to precisely determine indices of refraction of new optical materials such as Cs_2HgCl_4 that are under mechanical stress or influenced by an electric field [3,4]. The minimum intensity of light needed to perform measurements of optical properties is determined by the quantum nature of light and the desired precision of the optical parameter to be determined.

In order to determine both the material thickness and the index of refraction using single-wavelength photons, two experiments are performed. The first experiment uses a transmission based measurement in order to determine the material index of refraction that is independent of material thickness. The second experiment performs a transmission based interferometric experiment that is dependent upon both the index of refraction and the material thickness. The index of refraction is determined from parallel polarized single-photon transmission data for different angles of incidence using a curve fit to the Fresnel equations. The parallel polarization was chosen to normalize the photon counts at the Brewster angle. The equation for the optical path length change due to rotating a microscope coverslip is derived. This equation is used in conjunction with the index of refraction found in the first experiment to determine the material thickness from a second polarization based single-photon calcite polarization interferometer experiment. The resulting bit resolution and signal-to-noise ratio (SNR) in determining these macroscopic properties is discussed and compared with analog-to-digital converters (ADC) as a function of the number of photons received.

2. Experimental setup

The overall setup of the experimental apparatus is depicted in Figure 1. The source of single photons begins with a 50 mW 405 nm laser diode. This light is passed through a rotatable half-wave plate and then through a polarization beam splitter (PBS) that passes the horizontal polarization. Type I non-collinear down-converted photons are created when this light passes though a 0.5 cm thick type I BBO down-conversion crystal [5]. The reason for using the down-converted photons is that 814 nm is a common wavelength used in down-conversion experiments. Studying the index of refraction at this wavelength is useful when these new optical materials are used in down-conversion experiments. The resulting vertically

*Corresponding author. Email: jinwang@umd.umich.edu

ISSN 0950–0340 print/ISSN 1362–3044 online

http://dx.doi.org/10.1080/09500340.2011.628762
http://www.tandfonline.com

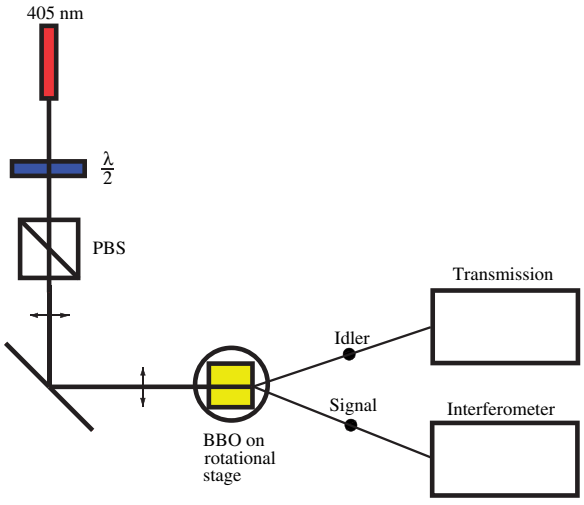

Figure 1. This figure depicts the overall layout of the experimental apparatus. The source of single photons for the transmission and interferometer experiments consists of a 405 nm laser diode, a 405 nm half-wave plate mounted on a rotatable mount, a polarizing cube beam splitter and a type I BBO down-conversion crystal. The half-wave plate and polarizing beam splitter are used to control the amplitude and polarization of the driving laser incident on the BBO crystal. (The color version of this figure is included in the online version of the journal.)

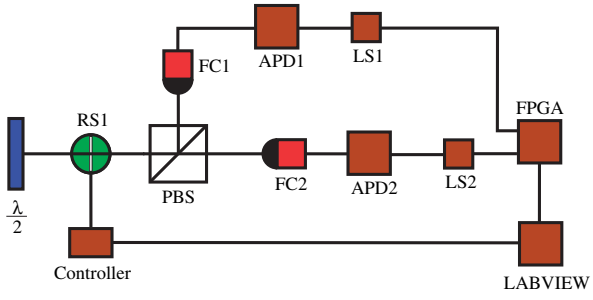

Figure 2. The setup for carrying out the single-photon transmission experiment is depicted in this figure. The vertically polarized idler beam passes through an 810 nm half-wave plate. This rotates the linear polarization by 45° which creates an equal amount of horizontally and vertically polarized photons. This light is incident on a microscope coverslip mounted to an automated rotational stage. The angle of incidence is controlled by a Labview^{TM} program running on a Personal Computer (PC). The photons are then split at a polarizing beam cube into horizontal and vertical components. These are collected into separate multimode fiber optics, detected using APDs, counted with an FPGA, then summed and recorded over four-second intervals with a PC. (The color version of this figure is included in the online version of the journal.)

polarized idler and signal photons from the BBO crystal are used to conduct both the single-photon transmission and interferometer experiments. In the transmission experiment depicted in Figure 2, the idler

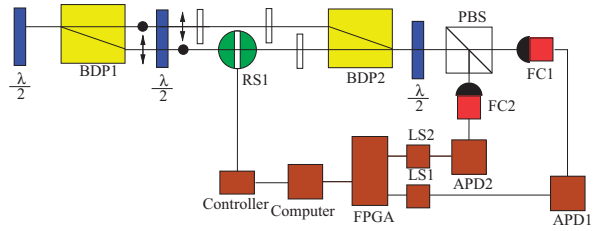

Figure 3. The interferometer setup uses a 810 nm half-wave plate held by a rotational mount to rotate the vertically polarized signal photons to 45°. The photons then travel through a BDP which separates the horizontal and vertical components by 3 mm. The 810 nm half-wave plate flips the polarization of the photons by 90°. The photons on the horizontally polarized upper arm traverse two coverslips that are oriented at a fixed angle. The vertically polarized photons on the lower arm traverse the coverslip mounted to an automated rotational stage and a coverslip at a fixed angle. Photons from both arms are then recombined with a second BDP. The photon polarization is rotated 45° before being separated into horizontal and vertical components at the PBS. The photons are then detected using APD detectors. The detection pulses representing single photons from the APD are sent through a level shifter then counted by an FPGA. The counts are then transferred to a program which sums and records the counts. The program, written in LabVIEW^{TM}, also controls the angle of the automated rotational stage. (The color version of this figure is included in the online version of the journal.)

photons first pass through a half-wave plate oriented at +22.5° to shift the polarization to +45°. The idler photons then traverse through a microscope coverslip and a PBS. After the PBS the polarization separated photons are launched into multimode fibers using fiber optic collimators. After traversing the fiber optic cable, the photons are then detected using two avalanche photodiode detectors (APD). The number of detected idler photons is counted by a Field Programmable Gate Array (FPGA). The angle of incidence of the photons with respect to the coverslip ϕ_i is varied from −70° to +70°, and counts are summed and recorded for each fixed angle over four-second intervals using Labview^{TM} and an automated rotational stage. The Fresnel equations [6] are curve fitted to the experimental results in order to find the index of refraction of the coverslip.

The second experimental section used to collect the interferometric data [7] is depicted in Figure 3. A half-wave plate changes the polarization of the signal photons from 90° to 45°. The photons are then passed through a calcite beam displacement prism (BDP) which separates the vertically and horizontally polarized components into two parallel paths that are separated by a horizontal distance of approximately 3 mm. The polarized components are then passed through a half-wave plate that flips their polarization

by 90°. The horizontally polarized component is passed through a coverslip to compensate for the distance increase due to the coverslip that is to be measured in the path with the vertically polarized component. Two additional rotatable coverslips are added in the vertically and horizontally polarized light paths in order to compensate for different BDP optical lengths and obtain better fringe visibility. The two polarization paths are then recombined at the second BDP and then passed through a half-wave plate to rotate the polarization by 45°. The signal photons are then counted and recorded in the same manner as in the transmission experiment. The angle of incidence ϕ_i of the single photons with respect to the coverslip is varied from −40° to +40°, and counts are collected at each angle for 1 second. A microscope coverslip was chosen for this experiment because it translates the beam an order of magnitude less than a microscope slide as it is rotated. By minimizing the translation of the beam, the variation in the detected number of photons due to the rotation angle is minimized. The variation in measured intensity is due to photons being missed by the fiber couplers as the beam is translated off center by the rotating coverslip.

3. Experimental results

Some theoretical background and experimental results of the transmission and interferometer experiments are discussed below. First, the transmission experiment is used to determine the index of refraction of the coverslip. By determining the index of refraction, the sample thickness can be found using the experimental data from the interferometer experiment.

The normalized experimental results from the transmission experiment along with the theoretical model are presented in Figures 4 and 5. The Fresnel model [6] for the transmission of polarized light parallel to the plane of incidence through the front and back surfaces of the sample T_{parallel} is given by:

$$T_{\text{parallel}} = 1 - \frac{\left(n_{\text{sample}}\cos(\phi_i) - \sqrt{1 - \frac{\sin^2(\phi_i)}{n^2_{\text{sample}}}}\right)^2}{\left(n_{\text{sample}}\cos(\phi_i) + \sqrt{1 - \frac{\sin^2(\phi_i)}{n^2_{\text{sample}}}}\right)^2}. \quad (1)$$

In Equation (1), n_{sample} represents the index of refraction of the sample, and the index of refraction of air is taken to be 1.0. In Figure 4, the maximum transmission of 100% occurs at around ±56.0° (Brewster's angle). The trough corresponds to an angle of incidence ϕ_i of zero. The average standard deviation of the transmission coefficient for each sample point is found to be 1.3×10^{-3} by subtracting the fitted theoretical curve

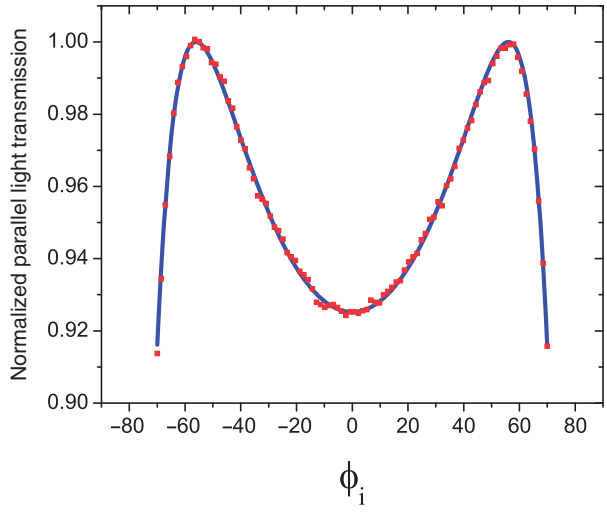

Figure 4. This figure shows the normalized experimental transmission results (dots) and a curve fit (solid) of the theoretical transmission of light parallel to the plane of incidence. (The color version of this figure is included in the online version of the journal.)

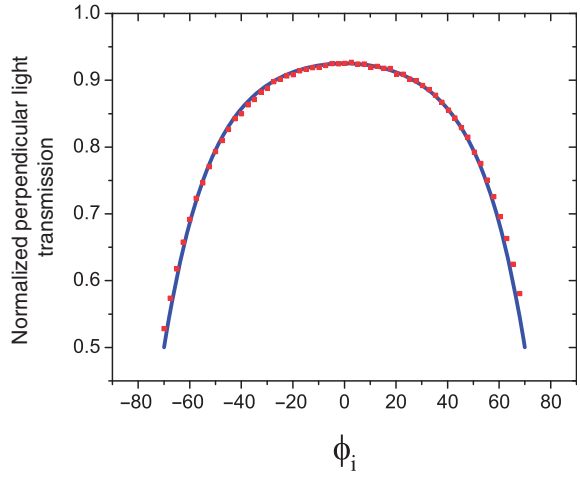

Figure 5. This figure shows the experimental (dots) and theoretical (solid) transmission amplitude of idler photons that have a polarization perpendicular to the plane of incidence. (The color version of this figure is included in the online version of the journal.)

from the experimental data. The SNR can be increased by curve fitting the theoretical Fresnel transmission to all the data points. By averaging together all 280 sample data points the standard deviation of the transmission will be reduced by $\sqrt{280}$ to 7.5×10^{-5}. This best curve fit of the transmission data yields an index of refraction of 1.485 with a standard deviation of 5.1×10^{-4}. The increase in the standard deviation is due to the nonlinear

relationship between the transmission measurements and the index of refraction as shown in Equation (1).

As a second check on how good an estimate of the index of refraction is, the experimental and theoretical transmission of light perpendicular to the plane of incidence is plotted in Figure 5 using the index of refraction determined by curve fitting light parallel to the plane of incidence. The amplitude of the transmitted photons is maximum for an angle of incidence of zero.

Since the index of refraction of the coverslip has been determined, the results of the interferometer experiment can now be used to find the thickness of the coverslip. The system model for the intensity of light detected consists of adding the amplitude of the stationary arm to the amplitude of the arm that changes. The amplitude of each arm is modeled using a cosine function. The phase of the arm with the rotating coverslip is given by ϕ_{rot}. The additional angle ϕ_{offset} compensates for a non-zero phase offset due to the path difference between the two arms when the angle of incidence ϕ_{i} is zero. The number of photons that are expected to be detected at APD1 is given by:

$$I_{\text{APD1}} = \cos^2(\phi_{\text{offset}} + \phi_{\text{rot}}). \tag{2}$$

The phase ϕ_{rot} is due to the change in the optical path length due to the rotating coverslip. The geometry of a ray of light passing through a coverslip of thickness d_{sample} at an angle ϕ_{i} is illustrated in Figure 6.

The interference pattern is caused by the change in the optical path length due to the rotating coverslip. The optical path length change leads to a change in the phase ϕ_{rot} of the light traversing the coverslip. The path length at normal incidence is given by P_{norm} in Equation (5). The path length when the coverslip is rotated by an angle ϕ_{i} is given by P_{rot} in Equation (6).

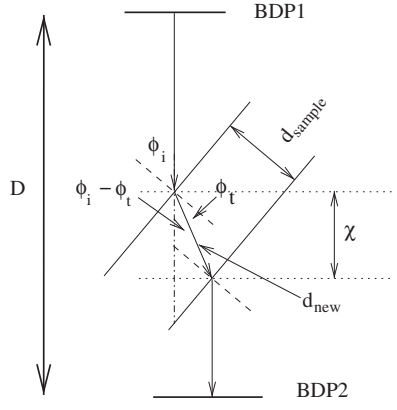

Figure 6. The geometry involved with deriving the optical path length difference when rotating the coverslip in one of the interferometer arms.

The optical path length taken by a ray of light through the coverslip is represented as d_{new} in Equation (3). The distance a ray of light travels through the coverslip parallel with the incident ray of light is represented by χ in Equation (4).

$$d_{\text{new}} = \frac{d_{\text{sample}}}{\cos(\phi_t)} \tag{3}$$

$$\chi = d_{\text{sample}} \cdot \frac{\cos(\phi_{\text{i}} - \phi_t)}{\cos(\phi_t)} \tag{4}$$

$$\text{P}_{\text{norm}} = (D - d_{\text{sample}}) + n_{\text{sample}} \cdot d_{\text{sample}} \tag{5}$$

$$\text{P}_{\text{rot}} = [D - \chi] + n_{\text{sample}} \cdot d_{\text{new}} \tag{6}$$

$$\phi_{\text{rot}} = \frac{2\pi}{\lambda}(\text{P}_{\text{norm}} - \text{P}_{\text{rot}}). \tag{7}$$

The physical distance occupied by the coverslip is represented by D. The angle of the transmitted light in the coverslip is represented by ϕ_{t}.

Equation (8), similarly to the Fendley paper [8], describes how the change in the optical path length creates a change in optical phase verses rotational angle ϕ_{i}. The change of the optical path length is calculated by subtracting Equation (6) from Equation (5).

$$\phi_{\text{rot}} = \frac{2\pi d_{\text{sample}}}{\lambda}\left[1 - \cos(\phi_{\text{i}}) - \frac{\sin^2(\phi_{\text{i}})}{n_{\text{sample}} \cdot \sqrt{1 - \frac{\sin^2(\phi_{\text{i}})}{n_{\text{sample}}^2}}}\right]$$
$$+ \frac{2\pi}{\lambda} n_{\text{sample}} \cdot d_{\text{sample}} \cdot \left[\frac{1}{\sqrt{1 - \frac{\sin^2(\phi_{\text{i}})}{n_{\text{sample}}^2}}} - 1\right]. \tag{8}$$

Here ϕ_{rot} is the phase difference in the arm with the coverslip as a function of the coverslip angle of incidence ϕ_{i}, and d_{sample} is the thickness of the coverslip. The phases ϕ_{rot} and ϕ_{offset} can be determined from the intensity of the experimental interference pattern. The sample's index of refraction n_{sample} was determined by the transmission experiment. The sample thickness d_{sample} can now be determined by performing a curve fit on the data from the interferometer experiment in Figure 7.

In Figure 7 the experimental results from the interferometer obtained at the horizontal polarization detector are compared with the best fit theoretical model curve using Equations (2) and (8). The peaks and troughs are the result of constructive and destructive interference in the two arms of the interferometer.

As the coverslip is rotated away from $\phi_i = 0^\circ$, the optical path length of the light going through it is increased as depicted in Figure 6. The interference pattern is the widest around $\phi_i = 0^\circ$ with the first nulls at -6.7° and 7.12°. The reason the fringes are closer together as the coverslip angle ϕ_i increases is that the optical path change per degree increases as ϕ_i increases. The maximum fringe visibility of the raw unscaled data is 0.75. The effect of the finite coherence length of the down-converted photons causes the visibility of the experimental fringe pattern in Figure 7 to diminish as the path difference between the two interferometer arms is increased.

The parameters ϕ_{offset} and ϕ_{rot} are determined from the experimental intensity illustrated in Figure 7 and curve fitting Equations (2) and (8). The sample thickness d_{sample} is determined by substituting n_{sample} from the transmission experiment into Equation 8. This results in a coverslip thickness d_{sample} of 160.4 μm with a standard deviation of 1.3 μm.

One additional result is that the relative phase difference between the two arms of the interferometer can be determined from fitting the experimental data. In this case it is found to be $\phi_{offset} = 13.4^\circ$. The slight offset in the angle of incidence due to misalignment of the perpendicular angle of incidence ($\phi_i = 0$) is 0.207°.

4. Discussion and summary

An advantage of using single-photon detection is that the effective resolution and signal-to-noise ratio (SNR) of the measurements are logarithmically proportional to the number of photons received. The APD can be considered a single-bit analog-to-digital converter (ADC) since it can only detect the presence or absence of a single photon. In Figure 4 the maximum number of photons received per sample is 855 344, and the effective bit resolution is given by $1 + \log_4(855\,344) = 10.8$ bits, or around 0.05% of the normalized data. This leads to a convenient way of increasing the effective bit resolution of the measured data from the field of digital signal processing called oversampling and decimation [9]. To increase the bit resolution by a single bit, simply acquire four times more photons. Or, equivalently, the SNR is doubled for every increase of one bit. The conclusion of this is that by using single-photon measurements, the effective resolution and SNR of the experimental results is only limited by the sample time.

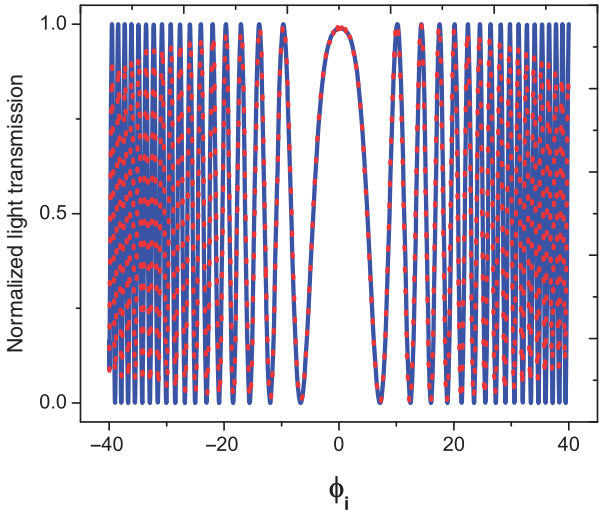

Figure 7. The theoretical (solid) and experimental (dots) results of the interferometer experiment. (The color version of this figure is included in the online version of the journal.)

In summary this paper has demonstrated the measurement of the optical parameters of index of refraction and material thickness using a quantum limited light source. The intensity used in the Fresnel experiment was 52 femtowatts. This is far below the accepted safe amount of laser radiation that can be accepted in the human eye [10]. Single-photon interferometry can have an increased resolution given enough time to collect the sample data. The measured light transmission found in the transmission and interferometer experiments has a standard deviation on the order of 0.13% for each data point. The optical parameters found have standard deviations on the order of 0.05%. The experimental precision and accuracy are found to increase as the number of detected photons is increased. This method of determining optical parameters at the quantum level may be useful in performing non-destructive measurements of light-sensitive materials with high precision.

Acknowledgements

The authors acknowledge the support of, and valuable discussions with, Vaman Naik, Jeffrey Prentis, Donald Bord, and Mark Beck. The authors recognize the contributions from Justin Opfermann, Gabe Elghoul, and Marwan Shoukair. The authors would also like to thank the OVPR and Rackham foundations from the University of Michigan for their support.

References

[1] Andrushchak, A.S.; Tybinka, B.V.; Ostrovskij, I.P.; Schranz, W.; Kityk, A.V. *Opt. Lasers Eng.* **2008,** *46,* 162–167.

[2] Yeh, Y.-L. *Opt. Lasers Eng.* **2008,** *46,* 197–202.

[3] Kaidan, M.V.; Zadorozhna, A.V.; Andrushchak, A.S.; Kityk, A.V. *Appl. Opt*. **2002,** *41,* 5341–5345.
[4] Andrushchak, A.S.; Mytsyk, B.G.; Demyanyshyn, N.M.; Kaidan, M.V.; Yurkevych, O.V.; Solskii, I.M.; Kityk, A.V.; Schranz, W. *Opt. Lasers Eng*. **2009,** *47,* 31–38.
[5] Kwiat, P.G.; Steinberg, A.M.; Chiao, R.Y.; Eberhard, P.H.; Petroff, M.D. *Phys. Rev. A* **1993,** *48,* R867–R870.
[6] Hecht, E. *Optics*, 4th ed..; Addison Wesley: Reading, MA, 2001.
[7] Gogo, A.; Snyder, W.D.; Beck, M. *Phys. Rev. A* **2005,** *71,* 052103.
[8] Fendley, J.J. *Phys. Educat*. **1982,** *17,* 209–211.
[9] Hauser, M.W. *J. Audio Eng. Soc*. **1991,** *39,* 3–26.
[10] Hallett, P.E. *J. Opt. Soc. Am. A* **1987,** *4,* 2330–2335.